Viscous Dissipation Effect on Magnetohydrodynamics Fluid Flow Over an Exponential Surface with the Influence of Thermal Radiation and Thermal Diffusion

Bayo Johnson Akinbo* and Bakai Ishola Olajuwon

Department of Mathematics, Federal University of Agriculture, Abeokuta, Nigeria
E-mail: akinbomaths@gmail.com
**Corresponding Author*

Received 26 December 2022; Accepted 11 March 2023;
Publication 29 April 2023

Abstract

This present investigation studies the effect of viscous dissipation in magnetohydrodynamics fluid flow over an exponential surface subject to the influence of thermal radiation and thermal diffusion. The coupled nonlinear guiding equations responsible for the flow, heat and mass transports presented as partial differential equations are revamped to the associated ordinary differential equation by application of the associated similarity variables and solved by Galerkin Weighted residual method (GWRM). The results of various parameters encountered are analyzed with graphs while the Sherwood number, Nussetl number, and local skin friction are computed and discussed. The study demonstrates, among other things, that the fluid has a strong thermal conductivity at low Prandtl numbers and that heat diffuses from the surface more quickly at low Prandtl numbers in comparison with the higher values.

Keywords: Heat sink/source, thermal radiation, thermal diffusion, Galerkin Weighted residual method.

European Journal of Computational Mechanics, Vol. 31_5–6, 583–600.
doi: 10.13052/ejcm2642-2085.31562

1 Introduction

The phenomenon of boundary layer flow of the continuous stretching sheet has great importance in manufacturing industries such as; wire drawing, paper production, metal rolling, drawing of plastic film, and metal spinning e.t.c. The foundational knowledge of the study was first reviewed by Sakiadis [1] while working on the boundary layer flow over a continuous stretching surface with constant speed and other authors like Crane [2], Carragher and Crane [3] and Wang [4] contributed widely to the literature with the early investigation. Due to its many industrial uses, it has gained scientific interest and received much study in the literature. Magyari and Keller [5] studied the flow of heat and mass transfer across an exponentially stretched continuous surface, using an analytical method and numerical solution. Partha et al. [6] justified that the thickness of the thermal boundary layer declines under the enhanced influence of the mixed convection parameter while working on a surface that is exponentially stretching with convection heat transfer in the part of laminar flow. El-Aziz [7] investigated the impact of viscous dissipation on micropolar fluid through an exponentially stretching sheet. The finding observed for forced convective flow alone, that variation in the micropolar parameter causes a higher rate of cooling of the sheet. Other authors like (Nadeem et al. [8, 9], Sanjayanand and Khan [10], Seini and Makinde [11], Bidin and Nazar [12]) worked on exponential stretching surface or sheet and their results agreed with the literature.

Some works had also been carried out on the exponentially stretchable sheet with the inclusion of the porosity parameter which is subject to vast industrial application as mentioned above. In the presence of thermal radiation, Sharma and Gupta [13] conducted an analytical study on MHD boundary layer flow and heat transport via a porous exponential stretchable surface. The result shows among other results obtained that the shear stress at the surface improved with the enhanced permeability which consequently magnified the temperature field within the boundary layer. A porous medium with an exponentially stretching porous sheet was the subject of Mandal and Mukhopadhyay's [14] investigation into the heat transport phenomenon of fluid flow, while Olumide et al. [15] investigated the combined effects of thermal radiation, heat absorption, and viscous dissipation on transport phenomena of heat and mass through an exponentially stretchable porous sheet. Other researchers such as Ahmad et al. [16], Singh [17] and Mukhopadhyay et al. [18] extended their findings with the inclusion of porosity parameter in the literature.

Motivated by the above work down, this study is being conducted to look at the significance of viscous dissipation on Magnetohydrodynamics fluid flow through an exponential surface under the influence of thermal radiation and thermal diffusion via Galerkin Weighted Residual Technique. The dynamics of different embedded parameters are plotted and discussed accordingly.

2 Mathematical Formulation

Considered here, is a stretching sheet steady-state with, momentum, thermal and mass boundary layers of two-dimensional layer flows. The plate has a surface temperature T_w and a surface concentration C_w whereas, the ambient temperature is presented as T_∞ as well as far-field concentration is taken as C_∞. The sheet is adopted to the variable magnetic force $B(x)$ utilized in a vertical trajectory to the flow while the induced magnetic appearance is disregarded due to the small magnetic Reynolds number. The coefficient of heat Source/sink is taken to be Q^* while the reaction rate is R. The steady flow governing equations of this study can be written as,

Continuity Equation;

$$\frac{\partial u}{\partial x} + \frac{\partial v}{\partial y} = 0 \tag{1}$$

Momentum Equation;

$$u\frac{\partial u}{\partial x} + v\frac{\partial u}{\partial y} = \nu\frac{\partial^2 u}{\partial y^2} - \frac{\sigma B^2(x)}{\rho}u \tag{2}$$

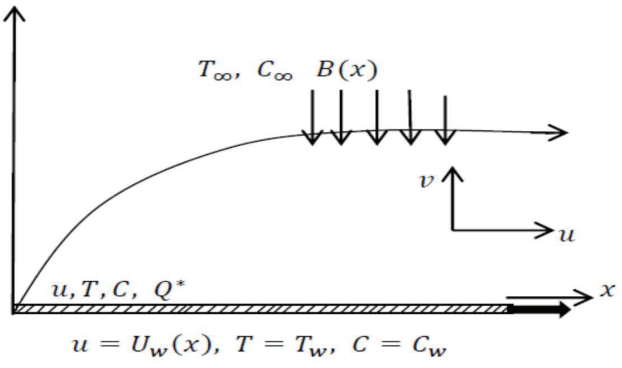

Figure 1 Flow configuration and coordinate system.

Energy Equation;

$$u\frac{\partial T}{\partial x}+v\frac{\partial T}{\partial y}=\frac{k}{\rho C_p}\frac{\partial^2 T}{\partial y^2}-\frac{1}{\rho C_\rho}\frac{\partial q_r}{\partial y}+\frac{\nu}{C_p}\left(\frac{\partial u}{\partial y}\right)^2+\frac{Q^*(T-T_\infty)}{\rho C_p} \tag{3}$$

Concentration equation

$$u\frac{\partial C}{\partial x}+v\frac{\partial C}{\partial y}=D_m\frac{\partial^2 C}{\partial y^2}+\frac{D_m K_T}{T_m}\frac{\partial^2 T}{\partial y^2}-R(C-C_\infty) \tag{4}$$

subject to the aforementioned assumption. In this case, (u, v) stands for the (x, y)-directional velocity components. The names of other notations are contained in the nomenclatures. The domain of the model

$$\begin{gathered} u=U_w=U_0e^{x/L},\quad v=0,\\ T=T_w=T_\infty+T_0e^{x/(2L)}\\ C=C_w=C_\infty+C_0e^{x/(2L)}\quad \text{at } y=0\\ u\to 0,\quad T\to T_\infty,\quad C\to C_\infty\quad \text{as } y\to\infty \end{gathered} \tag{5}$$

agreed with Noran et al. [19] and Seini and Makinde [11] while reference; temperatures, concentrations and length, are utilized as T_0, C_0 and L respectively. By using the Rosseland approximation, the radiative heat flux is condensed as

$$q_r=\frac{-4\sigma^*}{3k^*}\frac{\partial T^4}{\partial y} \tag{6}$$

Symbolically, σ^* conveys Stefan-Boltzmann constant, as k^* indicates the mean of absorption coefficient. Here, in accordance with Saqib et al. [20] as well as Akinbo and Olajuwon [21], the term T^4 can be stated as a linear function of temperature by expanding T^4 in a Taylor series, assuming that the temperature differences within the flow are such that

$$T^4=T_\infty^4T+4T_\infty^3(T-T_\infty)-6T_\infty^2(T-T_\infty)^2+\cdots \tag{7}$$

leaving out the higher order components in $(T-T_\infty)$ that go beyond the first degree, brings about

$$T^4\approx 4T_\infty^3T-3T_\infty^4 \tag{8}$$

Here, Equation (9) is the result of substituting Equations (8) and (6) in (3).

$$u\frac{\partial T}{\partial x}+v\frac{\partial T}{\partial y}=\left(\frac{k}{\rho C_{\rho}}+\frac{16\sigma^{*}T_{\infty}^{3}}{3k^{*}\rho C_{\rho}}\right)\frac{\partial^{2}T}{\partial y^{2}}+\frac{\nu}{C_{\rho}}\left(\frac{\partial u}{\partial y}\right)^{2}+\frac{Q_{0}(T-T_{\infty})}{\rho C_{\rho}} \tag{9}$$

By assuming the variable magnetic intensity $B(x)$ of the kind proposed by Seini and Makinde [11], we arrive at a similar solution.

$$B(x)=B_{0}e^{x/(2L)} \tag{10}$$

where B_0 is the magnetic intensity that is constant. Thus, Equation (1) is satisfied via the introduction of

$$u=\frac{\partial\psi}{\partial y}\quad\text{and}\quad v=-\frac{\partial\psi}{\partial x} \tag{11}$$

We obtained the transformed equations of the model in line with Seini and Makinde [11] and Anuar [22] by using

$$u=U_{0}e^{x/L}f'(\eta),\quad v=-\left(\frac{\nu U_{0}}{2L}\right)^{1/2}e^{x/(2L)}(f(\eta)+\eta f'(\eta)),$$

$$\eta=\left(\frac{U_{0}}{2\nu L}\right)^{1/2}ye^{x/(2L)},\quad T=T_{\infty}+T_{0}e^{x/(2L)}\theta(\eta)$$

$$C=C_{\infty}+C_{0}e^{x/(2L)}\emptyset(\eta) \tag{12}$$

on Equations (2), modified Equation (9) as well as Equations (4)–(5) result in

$$f'''(\eta)+f(\eta)f''(\eta)-\left(f'(\eta)\right)^{2}-Mf'(\eta)=0 \tag{13}$$

$$\left(1+\frac{4}{3}Ra\right)\theta''(\eta)+Prf(\eta)\theta'(\eta)-Prf'(\eta)\theta(\eta)$$

$$+PrEc(f''(\eta))^{2}+PrQ\theta(\eta)=0 \tag{14}$$

$$\emptyset''(\eta)+Scf\emptyset'(\eta)-Scf'(\eta)\emptyset(\eta)-Sc\beta\emptyset(\eta)+Sr\theta''(\eta)=0 \tag{15}$$

Which agreed with Noran et al. [19] and Seini and Makinde [11]. Here, $M=2\sigma B_{0}^{2}L/\rho U_{0}$ elucidates magnetic parameter, $Ra=4\sigma^{*}T_{\infty}^{3}/k^{*}k$ poses radiation parameter, $Pr=\nu\rho C_{\rho}/k$ is the Prandtl number, $Ec=U_{0}^{2}/T_{0}C_{p}$ presents Eckert number and $Sc=\nu/D_{m}$ indicates Schmidt number,

$\beta = 2LR/U_w$ forms chemical reaction and $Sr = T_0K_T/C_0T_m$ is the Soret number and $Q = Q_0L^2/U_0\rho C_p$ (See Hussain et al. [23]). The corresponding boundary conditions are as follows

$$f'(0) = 1, \quad f(0) = 0, \quad \theta(0) = 1, \quad \emptyset(0) = 1 \tag{16}$$

$$f'(\eta) \to 0, \quad \theta(\eta) \to 0, \quad \emptyset(\eta) \to 0 \quad \text{as } \eta \to \infty \tag{17}$$

3 Solution to the Problem

In applied mathematics, non-linear differential equations are frequently unavoidable. They are analyzed using many techniques, including the Homotopy Perturbation Method and Variation Iteration Method among others. Here, because the Galerkin Weighted Residual Method (GWRM) is effective at handling both linear and non-linear differential equations, it was chosen for this case. Razaq and Aregbesola [24] provided the precedent, and therefore considered basic trial functions of the form

$$f(\eta) = \sum_{i=0}^{12} a_i e^{-\frac{i\eta}{4}}, \quad \theta(\eta) = \sum_{i=1}^{13} b_i e^{-\frac{i\eta}{4}}, \quad \emptyset = \sum_{i=1}^{13} c_i e^{-\frac{i\eta}{4}} \tag{18}$$

Putting (16) in place, we have

$$\begin{aligned} &a_0 + a_1 + a_2 + a_3 + a_4 + a_5 + a_6 + a_7 + a_8 + a_9 + a_{10} \\ &\quad + a_{11} + a_{12} = 0 \end{aligned} \tag{19}$$

$$\begin{aligned} &b_1 + b_2 + b_3 + b_4 + b_5 + b_6 + b_7 + b_8 + b_9 + b_{10} + b_{11} \\ &\quad + b_{12} + b_{13} - 1 = 0 \end{aligned} \tag{20}$$

$$\begin{aligned} &c_1 + c_2 + c_3 + c_4 + c_5 + c_6 + c_7 + c_8 + c_9 + c_{10} + c_{11} \\ &\quad + c_{12} + c_{13} - 1 = 0 \end{aligned} \tag{21}$$

and for $f'(0) = 1$, we have

$$\begin{aligned} &-\frac{1}{4}a_1 - \frac{1}{2}a_2 - \frac{3}{4}a_3 - a_4 - \frac{5}{4}a_5 - \frac{3}{2}a_6 - \frac{7}{4}a_7 - 2a_8 - \frac{9}{4}a_9 \\ &\quad - \frac{5}{2}a_{10} - \frac{11}{4}a_{11} - 3a_{12} - 1 = 0 \end{aligned} \tag{22}$$

Thus, (17) is settled automatically. Also, invoking Equation (18) in Equations (13)–(15) resulted in residual functions R_f, R_θ and $R_\emptyset$ (See Akinbo

Table 1 Result analysis with Noran et al. [19]

						Noran et al. [19]			Present Results		
Ra	M	Pr	Sc	Q	β	$\lvert f''(0)\rvert$	$-\theta'(0)$	$-\emptyset'(0)$	$\lvert f''(0)\rvert$	$-\theta'(0)$	$-\emptyset'(0)$
0						1.912633	1.144381	0.586786	1.912620	1.144381	0.586776
1						1.912633	0.690717	0.586786	1.912620	0.690709	0.586776
2						1.912633	0.526667	0.586786	1.912620	0.526591	0.586776
	0					1.281933	0.753584	0.621791	1.281809	0.753562	0.621763
	1					1.629195	0.715307	0.600183	1.629178	0.715291	0.600160
	2					1.912633	0.690714	0.586782	1.912620	0.690709	0.586776
		1				1.912633	0.554890	0.586786	1.912620	0.690709	0.586776
		2				1.912633	0.873488	0.586786	1.912620	1.044676	0.586776
		3				1.912633	1.132214	0.586786	1.912620	1.326490	0.586776
			0.24			1.912620	0.293147	0.616260	1.912620	0.690709	0.616254
			0.62			1.912620	0.293147	1.051421	1.912620	0.690709	1.051421
			0.78			1.912620	0.293147	1.195670	1.912620	0.690709	1.195670
				0		1.912633	1.082728	0.690762	1.912620	0.398760	0.586776
				0.5		1.912633	1.241676	0.690762	1.912487	−1.455819	0.58669
				1.0		1.912633	1.373379	0.690762	1.912632	−0.43666	0.586776
					1	1.912633	0.690717	0.586786	1.912620	0.690709	0.586776
					2	1.912633	0.690717	0.766369	1.912620	0.690709	0.766369
					3	1.912633	0.690717	0.906532	1.912620	0.690709	0.906532

and Olajuwon [25, 26] for more details). The residual is multiplied by $e^{-\frac{j}{4}\eta}$, where $j \in \mathbb{Z}$, integrated under the appropriate domain. The MATHEMATICA package is used to solve the generated algebraic equations.

Validation of the model was ensured by comparing it with Noran et al. [19] for the local skin-friction, Nusselt Number and Sherwood number by setting $Ec = 0$, and $Sr = 0$. The findings were in line with one another as indicated in Table 1.

4 Discussion

Equations (13)–(15) constrain to (16) and (17) have been computed using the Galerkin Weighted Residual Method to gain a physical understanding of the issue. The resulting effects of various parameters are addressed accordingly. Also, the local skin-friction, Nusselt number, and Sherwood number in terms of $|f''(0)|$, $-\theta'(0)$ and $-\emptyset'(0)$, respectively were computed, for engineering applications. It is remarkable to note that the shear stress along the plate improves for large values of (M) which significantly boosts the local skin-friction and accelerates the flow. On the same hand, the Nusselt number gains strength as $Pr > 0$ and $Q > 0$. This in turns enhances the

Table 2 The skin-friction coefficient, local Nusselt number and local Sherwood number

M	β	Ec	Sr	Pr	Sc	Ra	Q	$\lvert f''(0)\rvert$	$-\theta'(0)$	$-\emptyset'(0)$
1								1.629178	0.295172	0.624503
3								2.158736	0.063548	0.621462
5								2.581130	−0.104279	0.623312
	1							1.629178	0.295172	0.624503
	3							1.629178	0.295172	0.957535
	5							1.629178	0.295172	1.192222
		1						1.629178	0.295172	0.624503
		3						1.629178	−0.289906	0.678011
		5						1.629178	−0.874984	0.731520
			0.1					1.629178	0.295172	0.624503
			0.5					1.629178	0.295172	0.601295
			1.0					1.629178	0.295172	0.572285
				0.72				1.629178	0.295172	0.624503
				1.0				1.629178	0.320056	0.624188
				3.0				1.629178	0.320976	0.630680
					0.24			1.629178	0.295172	0.624503
					0.62			1.629178	0.295172	1.072497
					0.78			1.629178	0.295172	1.219742
						1		1.629178	0.295172	0.624503
						2		1.629178	0.228782	0.626164
						3		1.629178	0.193045	0.627135
							0	1.629169	0.027577	0.640937
							0.3	1.629191	0.621207	0.626648
							0.8	1.632064	1.050596	0.599618

rate of heat transfer while the rate of mass transfer is boosted as Sherwood number increases on the account of large values of the chemical reaction and Schmidt number. (see Table 2).

When analyzing the model computationally, we varied each parameter as seen in the figures below while keeping $M = 1$, $Sr = 0.1$, $\beta = 1$, $Pr = 0.72$, $Sc = 0.24$, $Q = -0.5$, $Ra = 0.1$, $Ec = 0.1$ constant.

The dynamics of the magnetic parameter (M) on velocity and temperature fields are respectively illustrated in Figures 2 and 3. The outcome quantitatively meets expectations since increase in M causes greater resistance to the motion of the fluid, which reduces the thickness of the momentum layer. This phenomenon is subject to the presence of Lorentz force over in the variation in magnetic field. This force reduces the velocity field by acting against the motion of the fluid thereby reducing its movement. This may be

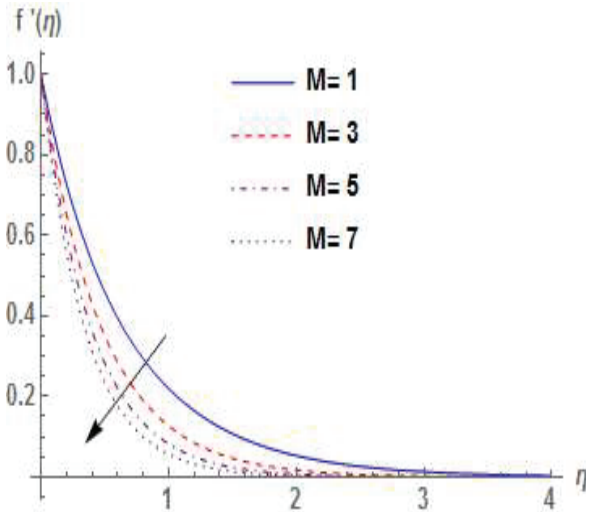

Figure 2 Effect of M on velocity field $f'(\eta)$.

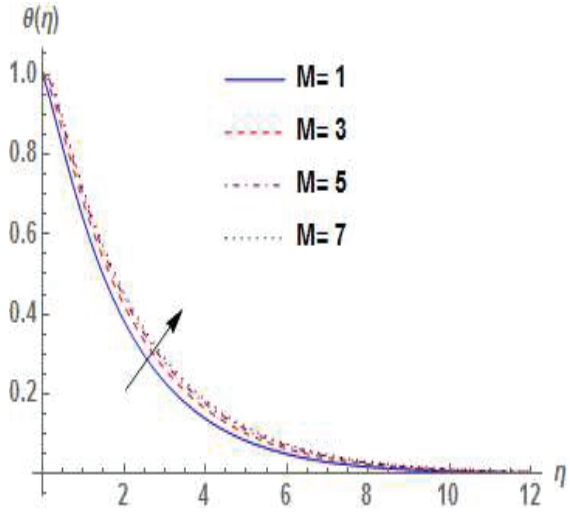

Figure 3 Effect of M on temperature field $\theta(\eta)$.

put to use in materials processing operations (Shahid et al. [27]), also essential for the boundary layer control in aerodynamics. In addition, the frictional heating that results from the interaction of M, subsequently increases the temperature field with a direct increasing impact on thermal boundary layer thickness.

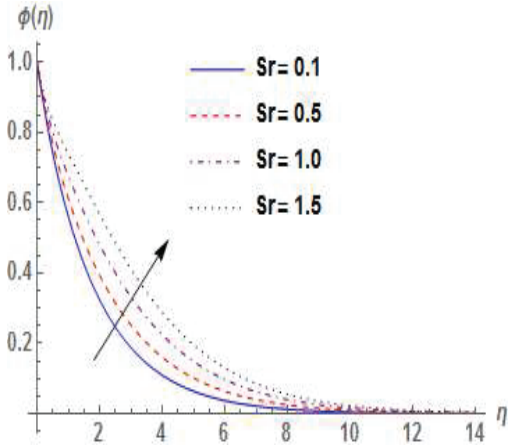

Figure 4 Effect of Sr on concentration field $\emptyset(\eta)$.

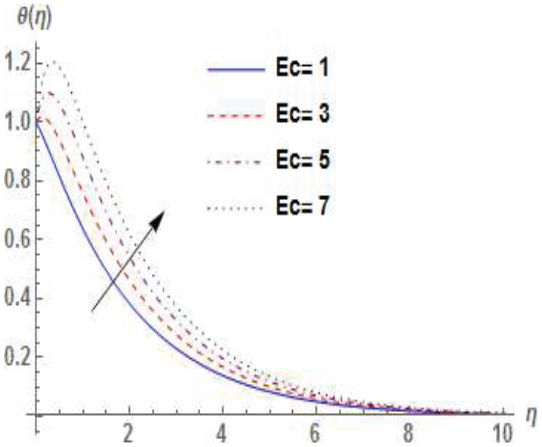

Figure 5 Effect of Ec on temperature field $\theta(\eta)$.

Figure 4 depicts the effect of Soret number (Sr) in concentration profile. The mass transport from lower to higher solute concentrations by temperature gradient is significantly influenced by the Soret effect (Hayat et al. [28]). A rise in Sr conveys the impact of temperature gradient on mass diffusion which strengthens the concentration field and boosts its boundary layer thickness.

The dynamics of Eckert number (Ec) which expresses a relationship between a flows kinetic energy and the boundary layer enthalpy is revealed in Figure 5. Higher variation on Ec enhances the temperature profile until it

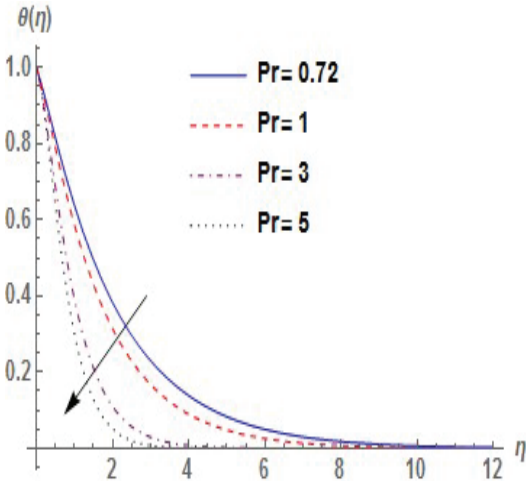

Figure 6 Effect of Pr on temperature field $\theta(\eta)$.

reaches its maximum value inside the boundary layer before abruptly falling monotonically and meeting the specifications for the distant field boundary conditions. To that end, an improvement in (Ec) indicates an increase in the rate of kinetic energy conversion to internal energy and the fluid close to the plate gets heated due to the heat addition caused by frictional heating, which raises the temperature field and the thickness of the thermal boundary layer that goes along with it (Koriko et al. [29]).

Figure 6 depicts the behaviours of Prandtl number $Pr(0.72,\ Air)$ in the temperature profile. An increase in Pr reduces the temperature field, together with the thickness of the thermal boundary layer. This result agreed with the literature as low values of Pr indicate that thermal diffusivity is dominant. However, when the values are large, the behaviour is dominated by the momentum diffusivity. For instance, the typical value for liquid mercury, which is around 0.025, shows that thermal diffusivity predominates because heat conduction is more significant than convection. When Pr is small, the heat diffuses more quickly than the higher values in the application.

Figure 7 illustrates the impact of Schmidt number (Sc) on the concentration field, discussed at the range of values 0.24(H_2), 0.62(H_2O), 0.78(NH_3) and 2.62(C_9H_{12}) for diffusing chemical species. Increase in Sc due to low molecular diffusivity results in rapid falls on the concentration profile. This outcome agreed with the expectation as inflation in Sc causes the momentum diffusion to dominate thereby suppressing the mass diffusion which consequently reduces the thickness of the concentration boundary layer.

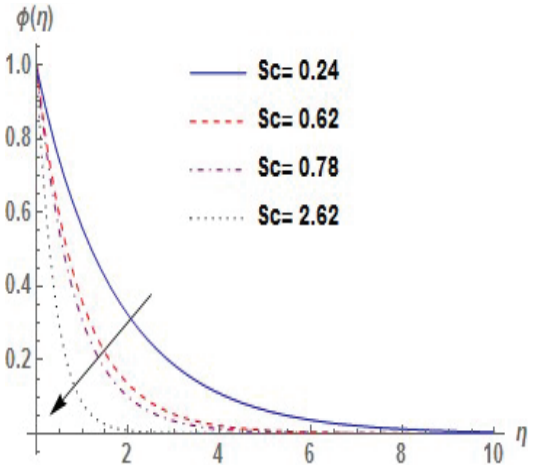

Figure 7 Effect of Sc on concentration field $\emptyset(\eta)$.

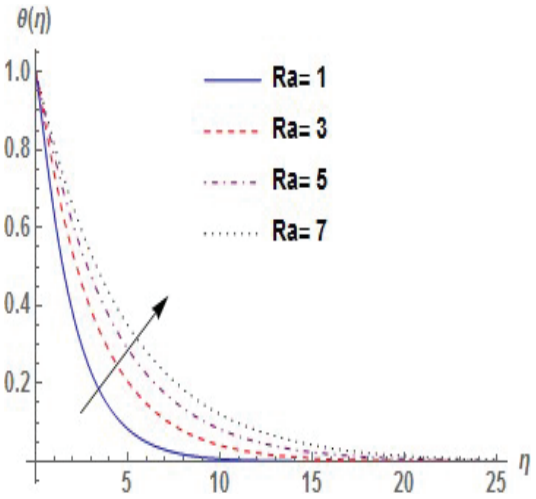

Figure 8 Effect of Ra on temperature field $\theta(\eta)$.

Figure 8 shows the influence of the radiation parameter (Ra) on the temperature profile. A rise in Ra causes a deterioration in the mean absorption coefficient thereby enhancing the temperature distribution across the boundary layer that consequently boosts the temperature field and strengthens the corresponding thermal boundary layer thickness.

Figure 9 presents the behaviours of the heat sink (Q) on the temperature profile. It is noticed that as $Q < 0$, the temperature profile ultimately declines

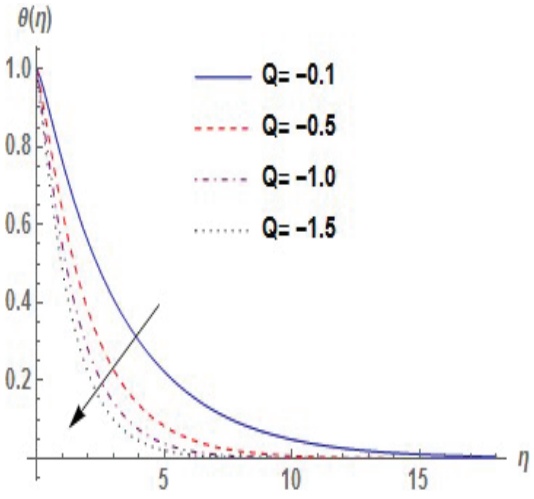

Figure 9 Effect of Q on temperature field $\theta(\eta)$.

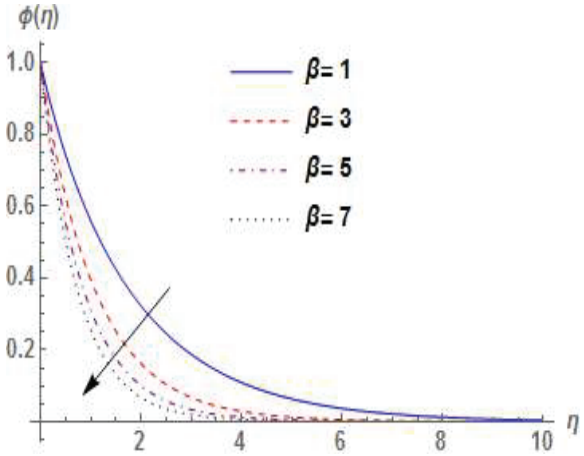

Figure 10 Effect of β on concentration field $\emptyset(\eta)$.

and consequently compresses the thermal layer thickness. This outcome agreed with the expectation as a rise in Q enhances cooling. This may be used for cooling of heat on the surface in Science related disciplines.

Figure 10 demonstrates the dynamics of chemical reaction (β) on the concentration field. A rise in β reduces the concentration buoyancy impact which consequently decreases the concentration of the fluid and lowers its layer thickness.

5 Conclusion

In this work, a steady-state two-dimensional boundary layer model has been carried out to investigate the viscous dissipation effect on magnetohydrodynamics fluid flow over an exponential surface in the presence of thermal radiation and thermal diffusion effect. Using the similarity method and the accompanying dimensionless variables, the resulting partial differential equations that characterize the problem are converted to dimensionless equations. We then solve the equations by Galerkin Weighted Residual Method (GWRM) and a comparison of the result with the previous work done shows a perfect agreement. At small values of Pr, fluid possesses high thermal conductivity and the heat diffuses away more quickly from the surface than higher values. Various values of (Sc), such as 0.24(H_2), 0.62(H_2O), 0.78(NH_3) and 2.62(C_9H_{12}) for most encountered chemical species in applications, diminishes the diffusion properties of the fluid of which its aftermath lowers the concentration layer thickness.

Nomenclatures

ν	Kinematic viscosity
ρ	Fluid density
k	Thermal conductivity
C_ρ	Specific heat at constant pressure
D_m	Mass diffusivity coefficient
q_r	Radiative heat flux
R	Reaction rate parameter
Q	Heat source/sink
T_m	Mean fluid temperature
T	Temperature
C	Concentration

References

[1] B. C. Sakiadis, Boundary-layer behaviour on continuous solid surfaces: I.Boundary-layer equations for two-dimensional and axi-symmetric flow. *American Institute of Chemical Engineering Journal*, **7**(1): 26–28, 1961. doi.org/10.1002/aic.690070108.

[2] L. J. Crane, Flow past a stretching plate. *Zeitschrift für angewandte Mathematik und Physik*, 21(4): 645–655, 1970. doi: 10.1007/BF0158 7695.

[3] P. Carragher, L. J. Crane, Heat transfer on a continuous stretching sheet. *Zeitschrift für Angewandte Mathematik und Mechanik*, 62(10): 564–573, 1982. doi.org/10.1002/zamm.19820621009.

[4] C. Y. Wang, The Three-Dimensional Flow due to a Stretching Flat Surface, *Phys. Fluids*, 27(8): 1915–1917, 1984. doi.org/10.1063/1.864868.

[5] E. Magyari, B. Keller, Heat and mass transfer in the boundary layers on an exponentially stretching continuous surface. Journal of Physics D: Applied Physics, 32(5): 577–585, 1999. doi.org/10.1088/0022-3727/32/5/012.

[6] M. K. Partha, P. V. S. N. Murthy, G. P. Rajasekhar, Effect of viscous dissipation on the mixed convection heat transfer from an exponentially stretching surface. *Heat and Mass Transfer*, 41(4): 360–366, 2005. doi: 10.1007/s00231-004-0552-2.

[7] M. A. El-Aziz, Viscous dissipation effect on mixed convection flow of a micropolar fluid over an exponentially stretching sheet. *Canadian Journal Physics*, 87(4): 359–368, 2009. doi.org/10.1139/P09-047.

[8] S. Nadeem, T. Hayat, M. Y. Malik, S. A. Rajput, Thermal radiation effects on the flow by an exponentially stretching surface. *Z. Naturforsch.*, 65a: 495–503, 2010. doi: 10.1515/zna-2010-6-703.

[9] S. Nadeem, S. Zaheer, T. Fang, Effects of thermal radiation on the boundary layer flow of a Jeffrey fluid over an exponentially stretching surface. *Numerical Algorithms*, 57(2): 187–205, 2011. doi: 10.1007/s11075-010-9423-8.

[10] E. Sanjayanand, S. K. Khan, On heat and mass transfer in a visco-elastic boundary layer flow over an exponentially stretching sheet. *International Journal of Thermal Science*, 45(8): 819–828, 2006. https://doi.org/10.1016/j.ijthermalsci.2005.11.002.

[11] Y. I. Seini, O. D. Makinde, MHD boundary layer flow due to exponential stretching surface with radiation and chemical Reaction. *Mathematical Problem in Engineering*, 1–7, 2013. http://dx.doi.org/10.1155/2013/163614.

[12] B. Bidin, R. Nazar, Numerical solution of the boundary layer flow over an exponentially stretching sheet with thermal radiation. *European Journal of Scientific Research*, 33(4): 710–717, 2009. http://www.europejournals.com/ejsr.htm.

[13] K. Sharma, S. Gupta, Analytical study of MHD boundary layer flow and heat transfer towards a porous exponentially stretching sheet in the

presence of thermal radiation. *International Journal of advance Applied Mathematics and Mechanics*, 4(1): 1–10, 2016.

[14] I. C. Mandal, S. Mukhopadhyay, Heat transfer analysis for fluid flow over an exponentially stretching porous sheet with surface heat flux in porous medium. *Ain Shams Engineering*, 4(1): 103–110, 2013. https://doi.org/10.1016/j.asej.2012.06.004.

[15] Olumide, J. Baiyeri, T. Ogunbayo, O. E. Enobabor, Thermal radiation and heat absorption effect on heat and mass transfer over an exponential stretching porous surface with viscous dissipation. *Asian Journal of Physical and Chemical Sciences*, 4(2): 1–9, 2017. doi: 10.9734/AJOPACS/2017/37260.

[16] I. Ahmad, M. Sajid, W. Awan, M. Rafique, W. Aziz, M. Ahmed, A. Abbasi, M. Taj, MHD flow of a viscous fluid over an exponentially stretching sheet in a porous medium. *Journal of Applied Mathematics*, 1–9, 2014. doi: 10.1155/2014/256761.

[17] A. K. Singh, Heat transfer and boundary layer flow past a stretching porous wall with temperature gradient dependent heat sink. *J.E.H.M.T.*, 28: 109–125, 2006.

[18] S. Mukhopadhyay, K. Bhattacharyya, G. C. Layek, Mass Transfer over an Exponentially Stretching Porous Sheet Embedded in a Stratified Medium. *Chemical Engineering Communications*, 201(2): 272–286, 2014. doi.org/10.1080/00986445.2013.768236.

[19] N. K. Noran, A. A. Samson, A. S. A. Aziz, Z. Md Ali, Chemical reaction and radiation effects on MHD flow past an exponentially stretching sheet with heat sink. *IOP Conference Series, Journal of Physics, Conf. Series*, 890: 012025, 2017. doi: 10.1088/1742-6596/890/1/012025.

[20] M. Saqib, F. Ali, I. Khan, N. A. Sheikh, Heat and mass transfer phenomena in the flow of Casson fluid over an infinite oscillating plate in the presence of first-order chemical reaction and slip effect. *Neural Computing and Applications*, 30(7): 2159–2172, 2018. doi: 10.1007/s00521-016-2810-x.

[21] B. J. Akinbo, B. I. Olajuwon, Impact of radiation and heat generation/absorption in a Walters' B fluid through a porous medium with thermal and thermo diffusion in the presence of chemical reaction. *International Journal of Modelling and Simulation*, 43: 87–100, 2023. doi.org/10.1080/02286203.2022.2035948.

[22] I. Anuar, MHD boundary layer flow due to an exponentially stretching sheet with radiation effect. *Sains Malays.* 40(4): 391–395, 2011.

[23] S. M. Hussain, R. Sharma, G. S. Seth, M. R. Mishra, Thermal radiation impact on boundary layer dissipative flow of Magneto-nanofluid over an exponentially stretching sheet. *International Journal of Heat and Technology*, 36(4): 1163–1173, 2018.

[24] A. O. Razaq, Y. A. S Aregbesola, Weighted Residual method in a semi-infinite domain using un-partitioned methods. *International Journal of Applied Mathematics*, 25(1): 25–31, 2012.

[25] B. J. Akinbo, B. I. Olajuwon, Convective heat and mass transfer in electrically conducting flow past a vertical plate embedded in a porous medium in the presence of thermal radiation and thermo diffusion. *Computational Thermal Sciences*, 11(4): 367–385, 2019. doi: 10.161 5/computthermalScien.2019025706.

[26] B. J. Akinbo, B. I. Olajuwon, Effects of Heat Generation/Absorption on Magnetohydrodynamics Flow Over a Vertical Plate with Convective Boundary Condition. *European Journal of Computational Mechanics*, 30(4–6): 431–452, 2021.

[27] A. Shahid, M. M. Bhatti, O. A. Bég, Numerical study of radiative Maxwell viscoelastic magnetized flow from a stretching permeable sheet with the Cattaneo–Christov heat flux model. *Neural Comput Appl.*, 30(11): 3467–3478, 2018.

[28] T. Hayat, T. Nasir, M. I. Khan, A. Alsaedi, Numerical investigation of MHD flow with Soret and Dufour effect. *Results in Physics*, 8: 1017–1022, 2018.

[29] O. K. Koriko, K. S. Adegbie, N. A. Shah, I. L. Animasaun M. A. Olotu, Numerical solutions of the partial differential equations for investigating the significance of partial slip due to lateral velocity and viscous dissipation: The case of blood-gold Carreau nanouid and dusty uid Numerical Methods for Partial Differential Equations, 37, 205–226, 2021.

Biographies

Bayo Johnson Akinbo (B.Sc.[Ed]., M.Sc., Ph.D) is a Researcher at Federal University of Agriculture, Abeokuta, Nigeria. His area of research involves Fluid Mechanics and Mathematical Modeling.

Bakai Ishola Olajuwon (B.Sc., M.Tech., Ph.D) is a Professor and Researcher at Federal University of Agriculture, Abeokuta, Nigeria. His area of research involves Fluid Mechanics and Mathematical Modeling.